

A Dependency of Quantum Efficiency of Silicon CMOS n^+pp^+ LEDs on Current Density

Lukas W. Snyman, *Member, IEEE*, Herzl Aharoni, *Senior Member, IEEE*, and Monuko du Plessis, *Senior Member, IEEE*

Abstract—A dependency of quantum efficiency of nn^+pp^+ silicon complementary metal–oxide–semiconductor integrated light-emitting devices on the current density through the active device areas is demonstrated. It was observed that an increase in current density from $1.6 \times 10^{+2}$ to $1.6 \times 10^{+4} \text{ A} \cdot \text{cm}^{-2}$ through the active regions of silicon n^+pp^+ light-emitting diodes results in an increase in the external quantum efficiency from 1.6×10^{-7} to 5.8×10^{-6} (approximately two orders of magnitude). The light intensity correspondingly increase from 10^{-6} to $10^{-1} \text{ W} \cdot \text{cm}^{-2} \cdot \text{mA}$ (approximately five orders of magnitude). In our study, the highest efficiency device operate in the p-n junction reverse bias avalanche mode and utilize current density increase by means of vertical and lateral electrical field confinement at a wedge-shaped n^+ tip placed in a region of lower doping density and opposite highly conductive p^+ regions.

Index Terms—Complementary metal–oxide–semiconductor (CMOS) technology, electroluminescence, light-emitting diodes (LEDs), silicon.

I. INTRODUCTION

A NEED for the development of electrooptical interfaces in large scale integration and very large scale integration complementary metal–oxide–semiconductor (CMOS) integrated circuitry has recently been expressed. [1]–[5]. Substantial research has been conducted in the field of electroluminescence from silicon utilizing fabrication techniques with amorphous silicon structures, Si superlattice structures and implantation of foreign species into silicon [6]–[10]. Many of these technologies utilize nonstandard processing procedures and cannot be easily integrated into the present standard CMOS integrated circuit technology. Light emission has been observed to be emitted from silicon devices that operate in the reverse

Manuscript received December 30, 2004; revised June 13, 2005. The subject of this work forms the content of the U.S. Patent 5 944 720, November 30, 1999, U.S. Patent Application 08/938, 730, August 29, 2000, and South Africa Patent 96/2528 and 96/2478, 1996 and 1998, respectively. This work was supported by the Department of Electronic Engineering, University of Pretoria, and by the Carl and Emily Fuchs Foundation in South Africa.

L. W. Snyman was with the Carl and Emily Fuchs Institute for Microelectronics (CEFIM), Department of Electrical, Electronic and Computer Engineering, University of Pretoria, Pretoria 0001, South Africa. He is now with the Department of Electronic Engineering, Tshwane University of Technology, Pretoria 0001, South Africa (e-mail: snymanlw@tut.ac.za).

H. Aharoni is with the Carl and Emily Fuchs Institute for Microelectronics (CEFIM), Department of Electrical, Electronic and Computer Engineering, University of Pretoria, Pretoria 0001, South Africa, and also with the Department of Electrical and Computer Engineering, Ben-Gurion University of the Negev, Beer-Sheva 84105, Israel.

M. du Plessis is with the Carl and Emily Fuchs Institute for Microelectronics (CEFIM), Department of Electrical, Electronic and Computer Engineering, University of Pretoria, Pretoria 0001, South Africa.

Digital Object Identifier 10.1109/LPT.2005.856448

TABLE I
DESIGN DETAILS AND PERFORMANCE CHARACTERISTICS AS MEASURED FOR VARIOUS SILICON CMOS AND BiCMOS ELECTROOPTICAL INTERFACE TEST STRUCTURES, AS DESIGNED BY SNYMAN *et al.*

Test structure and Reference	Device design and device dimensions	Active light emitting area	Test conditions	Measured optical output
TS1 ⁶	Seven segments displayed in 1.2 micron CMOS silicon n^+ planar design in p-well with guard ring protection	100 X 400 micron per segment	31 V 0.1 to 10 mA per segment	1.02 nW per mA of current
TS3 ¹⁸	Seven segments displayed in 2 micron Bi-CMOS silicon n^+ planar design in p-base well	30 X 215 micron per segment	8V 0.1 to 10 mA per segment	0.8nW per mA of current
TS4 ¹⁸	Circular optical fibre interface in 1.2 micron CMOS silicon n^+ planar design with perforated n^+ layer	60 micron diameter	31V 0.1 to 10 mA	0.6 nW per mA of current
TS5 ¹⁴	Circular optical fibre interface in 1.2 micron CMOS silicon n^+ circular ring structure in p well	20 micron diameter	4V 0.1 to 10 mA	5nW per mA of current
TS8 (See Fig. 3)	Point light source n^+ wedge embedded in p-base	1 micron diameter	8V 0.1 to 5 mA	1nW per 0.1 mA of current

bias avalanche mode of operation [11], [12]. Although initial versions of these devices revealed low electrical-to-optical power conversion efficiencies and quantum efficiencies (of the order of 10^{-9} and 10^{-8}), respectively, [12] they offer major advantageous in terms of ease of integration in standard state of the art silicon technology and in terms of a high-speed modulation capability (of the order of gigahertz). We have developed several new version of devices using conventional CMOS integrated circuit technology with increased power and quantum conversion efficiencies [13]–[18]. Table I summarizes the major characteristics of the devices and the major electrooptical characteristics as published to date by our group. Fig. 1 shows a photomicrograph of a 60- μm -diameter optical fiber interface (TS4) as realized with 1.2- μm bi-CMOS technology. The light emission level is $\sim 4 \times 10^{-4} \text{ W} \cdot \text{cm}^{-2}$ or about 1 nW for the area shown.

In this letter, a remarkable dependency of the quantum efficiency on the current density through the active regions of Si n^+pp^+ avalanche mode devices is illustrated. The results have been derived through recent extensive modeling and analyses of results which has been accumulated over some time. This observation may especially sheds some new understanding on the mechanisms controlling the light emission in these devices.

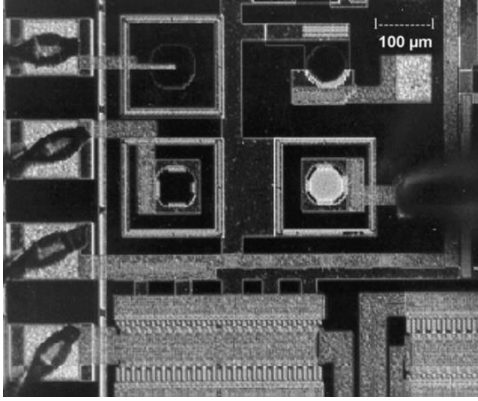


Fig. 1. Photomicrograph of a 60- μm -diameter optical fiber interface (TS4) as realized with 1.2- μm bi-CMOS technology. The light emission level is $\sim 4 \times 10^{-4} \text{ W} \cdot \text{cm}^{-2}$ or about 1 nW for the area shown.

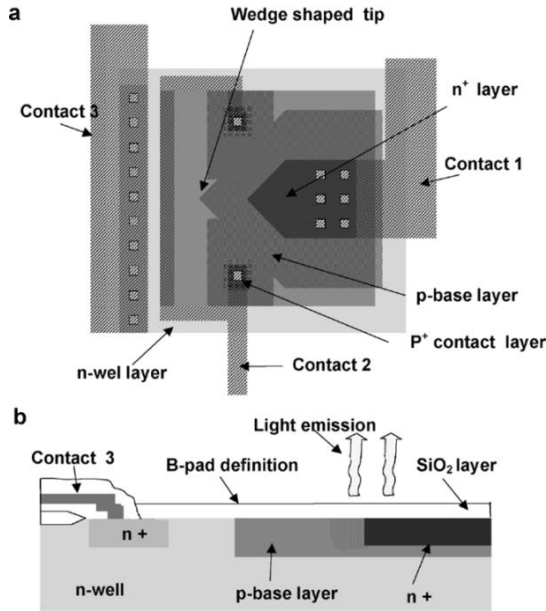


Fig. 2. Schematic planar layout and cross-sectional layout of shallow-junction planar $n^+ pp^+$ Si light emitting device using a 2- μm silicon CMOS technology with a bipolar capability.

II. GENERATION OF A HIGH CURRENT DENSITY, SURFACE-EMITTING CMOS Si LIGHT-EMITTING DIODE (LED)

In one of our latest designs, a test structure 8 (TS8), as illustrated in Fig. 2(a) and (b), an n^+ planar wedge-shaped body was embedded in a p-base bed, as utilized in Bi-CMOS technology fabrication process¹ and further placed opposite two bodies of p^+ regions. The n^+ and p^+ regions were created by ion implantation while the p-base region was created by means of boron gas diffusion. The maximum gradient in the doping density for this configuration is about 0.1 μm from the Si-SiO₂ interface. This implies that, when the n^+p junction is laterally reverse biased, the prevailing depletion region extends coplanarly with the Si-SiO₂ interface. If the bias is high enough, a

¹A 2- μm process with a bipolar capability, as offered by Orbit Inc., CA, 1996-2000.

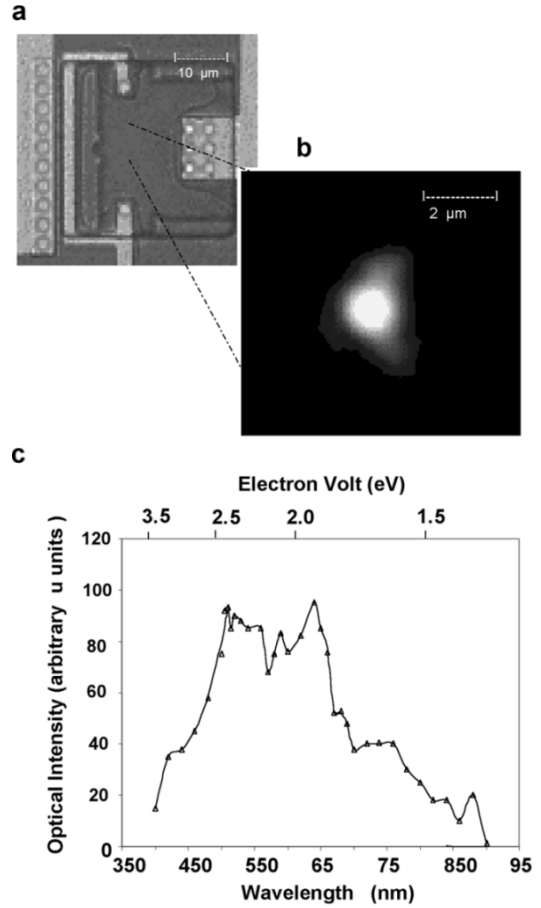


Fig. 3. (a) Photomicrograph of test structure 8 (TS8) and shallow-junction planar $n^+ pp^+$ Si light-emitting device using a 2- μm silicon CMOS technology with a bipolar capability. (b) Performance characteristics of the device under subdued ambient lighting conditions at 8 V and 0.1 mA. (c) Spectrographic data for the TS8-type structures.

process of avalanche occurs virtually at the Si-SiO₂ interface. Expected optical losses within the highly absorption silicon substrate is, therefore, minimized. The current density was further confined in a lateral direction to about a $2 \times 1 \mu\text{m}$ region by using a wedge-shape design for the n^+ layer, and appropriately placing two p^+ doped regions and ohmic metal contacts diagonally across the wedge-shaped tip [Fig. 2(a)]. This configuration enabled extremely high electric field confinement and extremely high current density at the tip of the n^+ wedge shape. The intensity of the light as emitted at the wedge-shaped could be appropriately modulated by putting positive bias on a third terminal contact placed in an n-well body [Fig. 2(a)].

Experimental measurements showed that light of very high brightness were emitted from the device in a very small 1- μm diameter, as illustrated in Fig. 3(a) and (b). Fig. 3(a) shows a bright field optical micrograph of the top surface device as outlined in Fig. 2, and Fig. 3(b) shows a dark field optical micrograph of an area on the device at higher magnification showing the characteristics of the light emission. The luminescence intensity were measured to be very high, reaching values of up to 1 nW per μm^2 . The operating conditions at this measurement were 8 V at only 80 μA of current. No detectable degradation in the optical output as associated with the device could be observed.

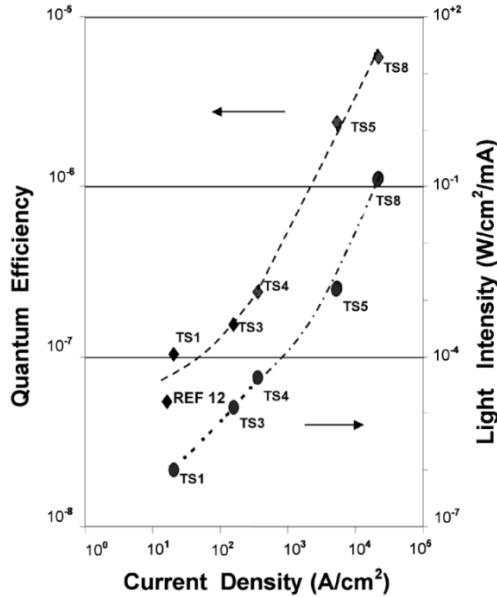


Fig. 4. Calculated normalized quantum efficiencies and measured light intensity as a function of current density through the active light-emitting areas of the devices for various silicon CMOS light-emitting test structures that operate in the reverse bias avalanche mode of operation.

III. CALCULATED QUANTUM EFFICIENCY AS A FUNCTION OF CURRENT DENSITY THROUGH THE ACTIVE LIGHT-EMITTING AREA OF THE DEVICES

From the measured optical output, the dimensions and test operating conditions for the various devices as listed in Table I, corresponding light intensities and external quantum efficiency and current densities could be calculated and compared with the results as obtained for TS8. The external quantum efficiency was derived from the relationship

$$N_Q = \frac{(e\lambda V)}{hc} N_p \quad (1)$$

where N_p denotes the power conversion efficiency, e denotes the elementary charge, λ the wavelength, V the applied voltage, h the Planck constant, and c the speed of light. This relationship represents the ratio of the number of photons emitted from the junction to the number of charge carriers that passed through the junction. The power conversion efficiency was calculated by dividing the externally measured optical output, by the applied total electrical power as applied to the device in terms of the current-voltage product.

Since the quantum efficiency according to (1) is dependent on operating voltage, and this operational condition varied from one device design to the other, the calculated quantum conversion efficiencies could be normalized with respect to this parameter to a standardized operating voltage of 8 V. The current density through the current conducting and avalanching area of TS8 were $\sim 4 \times 10^4 \text{ A} \cdot \text{cm}^{-2}$ as compared to the uniform current density of $\sim 2 \times 10^1 \text{ A} \cdot \text{cm}^{-2}$ as for in TS1 at 0.1 mA of current. The derived average and normalized quantum efficiencies and light intensities as measured for the devices in Table I together with that of TS8 are presented in Fig. 4. The results are compared with the initial results of Kramer *et al.* [12] which is shown on the graph as reference structure [12].

Fig. 4 reveals the following derivations: 1) A clear linear dependency of the normalized quantum efficiency as a function of current density through the active regions of the device. A relationship dependence of $n = 0.9$ is derived for the quantum efficiency as a function of current density using $\eta = a \cdot x^n$ power series analyzes. 2) A clear linear increases in the light intensity as a function of current density as emitted from the devices over about four orders of magnitude. 3) Indications of an inflection point for the quantum efficiency (i.e., higher than linear dependency) at a current density of about $6 \times 10^3 \text{ cm}^{-2}$.

The effect was also observed for increasing the current density through the active region of a single device, but could not be so explicitly observed due to limitations in the maximum current density and current carrying capability as associated with one particular device.

REFERENCES

- [1] D. A. Miller, "Silicon integrated circuits shine," *Nature*, vol. 384, pp. 307–308, 1996.
- [2] H. U. Habermeier, "E-MRS spring meeting in June to focus on electronic materials," *Mater. Res. Soc. Bull.*, vol. 23, no. 4, pp. 13–14, 1998.
- [3] E. A. Fitzgerald and L. C. Kimerling, "Silicon-based technology for integrated optoelectronics," *Mat. Res. Soc. Bull.*, vol. 23, no. 4, pp. 39–45, 1998.
- [4] D. J. Robbins, "Silicon opto-electronics," in *Proc. Int. Society for Optical Engineering (SPIE) and Photonic West Annu. Conf.*, vol. 3953, San Jose, CA, Jan. 2000.
- [5] N. Savage, "Holy grail—Light from silicon," *IEEE Spectr.*, vol. 41, no. 1, p. 59, Jan. 2004.
- [6] J. M. Baribeau, Z.-H. Lu, and D. J. Lockwood, "Visible light-emitting (Si/SiO₂) superlattices," *IEEE LEOS Newsletter*, vol. 10, no. 2, p. 4, 1996.
- [7] J. Stimmer, A. Reittinger, J. F. Nutzel, G. Abstreiter, H. Holzbrecher, and C. Buchel, "Electroluminescence of Erbium-oxygen-doped silicon diodes," *Appl. Phys. Lett.*, vol. 68, no. 23, pp. 3290–3292, 1996.
- [8] T. Taskin, Q. Huda, A. Scholes, J. H. Evans, A. R. Peaker, P. Hemment, C. Jeyens, and Z. Jafri, "Non-radiative competition in the excitation of erbium-implanted silicon light emitting devices," in *Proc. Thin Films for Integrated Optics Applications*. Pittsburgh, PA, 1996, pp. 223–228.
- [9] D. Leong, M. Harry, K. J. Reeson, and K. P. Homewood, "A silicon/iron-disilicide light emitting diode operating at a wavelength of 1.5 micron," *Nature*, vol. 387, pp. 686–688, 1997.
- [10] K. D. Hirschman, L. Tsybeskov, S. P. Duttagupta, and P. M. Fauchet, "Silicon-based visible light-emitting devices integrated into microelectronic circuits," *Nature*, vol. 384, pp. 338–341, 1996.
- [11] A. G. Ghyneweth and K. G. McKay, "Photon emission from avalanching breakdown in silicon," *Phys. Rev.*, vol. 102, pp. 369–376, 1956.
- [12] J. Kramer, P. Seitz, E. F. Steigmeier, H. Auderset, and B. Delley, "Industrial CMOS technology for the integration of optical metrology systems," *Sens. Actuators*, vol. A37–38, pp. 527–533, 1993.
- [13] L. W. Snyman, H. Aharoni, M. du Plessis, and R. B. J. Gouws, "Increased efficiency of silicon light-emitting diodes in a standard 1.2- μm silicon complementary metal oxide semiconductor technology," *Opt. Eng.*, vol. 37, pp. 2133–2141, 1998.
- [14] L. W. Snyman, M. du Plessis, E. Seevinck, and H. Aharoni, "An efficient low voltage, high frequency silicon CMOS light emitting device and electro-optical interface," *Electron Device Lett.*, vol. 20, pp. 614–617, 1999.
- [15] L. W. Snyman and A. Biber, "Enhanced light emission from a Si n⁺ pn CMOS structure," in *Proc. 1999 IEEE SoutheastCON 1999*, Lexington, KY, Apr. 1999, IEEE Cat No 99CH36300, ISBN 0-7803-5237-8, pp. 242–245.
- [16] L. W. Snyman, H. Aharoni, A. Biber, A. Bogalecki, L. Canning, M. du Plessis, and P. A. Maree, "Optical sources, integrated optical detectors and optical waveguides in standard CMOS integrated circuitry," in *Proc. SPIE Series and Photonic West Optoelectronics 2000 Conf.*, vol. 3953, San Jose, CA, Jan. 22–28, 2000, invited overview paper, pp. 20–36.
- [17] M. du Plessis, H. Aharoni, and L. W. Snyman, "Silicon light emitting devices in standard CMOS technology," in *Proc. IEEE Conferenta Anuala de Semiconductor (CAS)*, Romania, Oct. 2001, ISBN 07803-6666-2; IEEE Cat. 01TH8547 (invited paper), pp. 231–238.
- [18] L. W. Snyman, H. Aharoni, M. du Plessis, J. F. K. Marais, D. van Niekerk, and A. Biber, "Planar light emitting electro-optical interfaces in standard silicon complementary metal oxide semiconductor integrated circuitry," *Opt. Eng. (SPIE-USA)*, vol. 41, no. 12, pp. 3230–3240, Dec. 2002.